Spectroscopy and Photochemistry of *meso*-Diphenyltribenzonaphthoporphyrin at Low Temperatures: A Novel System for Hole-Burning Applications

Bernd Plagemann,* Indrek Renge,† Alois Renn, and Urs P. Wild

Physical Chemistry Laboratory, Swiss Federal Institute of Technology, ETH Zentrum, CH-8092 Zürich, Switzerland

Received: October 15, 1997; In Final Form: December 31, 1997

We present a custom-tailored material for the application of spectral hole-burning in optical storage and imaging spectroscopy. The photoactive molecule *meso*-diphenyltribenzonaphthoporphyrin (P_2TriBNP) combines the advantages of chlorins and simple porphyrins used so far, namely, the spectral separation between photoeduct and photoproduct states and a high photochemical hole-burning yield. Basic characteristics of the material were measured. We obtained the values of $3.2 \pm 1.5\%$ for the hole-burning yield, of ~ 0.6 for the Debye−Waller factor in poly(vinyl butyral) (PVB), and a spectral separation between the educt and product absorption of 120 cm^{-1}. The difference in the dipole moment between the ground and the excited state shows two contributions. The permanent dipole moment difference has a value of 0.29 ± 0.03 D. A root mean square value of 0.15 ± 0.02 D for a distributed, matrix-induced component was measured. Because of their high photochemical yields and the large absorption cross sections, P_2TriBNP and similar compounds open the way for a new class of experiments dealing with lower light intensities and shorter exposure times than before. However, we observed the lifetime of narrow spectral holes to be limited to several hours. Nevertheless, the material exhibits a high potential for the application in imaging spectroscopy, e.g., the simultaneous recording of spatial and spectral information of astronomical objects.

1. Introduction

Persistent spectral hole-burning (PSHB)[1−4] can be used for optical data storage with very high storage densities[5,6] as well as in high-resolution spectroscopy. The technique is well-established, and the holographic recording techniques and the readout and handling of the retrieved data have been optimized over the last years.[7−10] The promotion of this technology into practical applications calls mainly for the improvement of the material parameters of the systems used. In the following we concentrate on the description of the parameters that are crucial in this quest and their connection to the structure of the investigated molecules.

1.1. Hole-Burning Parameters. The main advantage of PSHB materials is the very high frequency selectivity which should be maintained when searching for new compounds. As a continuation of the improvements in PSHB materials,[11,12] we concentrate in this paper on the optimization of the hole-burning quantum yield. This parameter is crucial to have in practical applications since it limits the obtainable recording speeds and necessary light levels. So far, mainly two classes of materials have been used for a hole-burning memory: inorganic crystals doped with rare-earth ions and organic dye molecules doped into polymers. The inorganic systems are generally advantageous in the ratio of inhomogeneous to homogeneous line width. However, the dye-doped polymers have significantly larger absolute values of the hole width on the order of some hundred megahertz, which makes them much better suited for the use with commercially available light sources like single-mode lasers. The scope of this investigation is restricted to the latter case of dye-doped polymers, or specifically a porphyrin analogue, *meso*-diphenyltribenzonaphthoporphyrin (P_2TriBNP) in PVB.

The main parameters that determine the applicability of the chromophore−host systems for optical data storage using PSHB and other hole-burning applications are the frequency selectivity, the hole-burning efficiency, and the stability of the spectral holes.[3]

The frequency selectivity is characterized by the ratio of the inhomogeneous to the homogenous line width of the molecular absorption, which corresponds to the transition between the singlet ground state and the first excited state. The homogeneous line width is determined by the lifetime and the phase relaxation times of the excited state.[3] The phase relaxation time is temperature-dependent.[13] At room temperature, the amount of homogeneous broadening is similar to the inhomogeneous contribution, and therefore, the ratio is close to 1. For liquid nitrogen temperatures, recent investigations[14] indicate a value for the ratio as high as 10^2. At liquid helium temperatures, the ratio of inhomogeneous to homogeneous broadening, which can specify the amount of the obtainable storage density, is typically as high as 10^4-10^5.

Recent investigations have explored the use of PSHB for ultrahigh-density data storage and imaging spectroscopy.[15−17] The main obstacle in these applications was the low hole-burning efficiency of the system used, chlorin in PVB. In holographic data storage applications, this resulted in the minimum exposure time for a single page of data to be on the order of seconds.[15] Furthermore, the simultaneous recording of spectral and spatial information of astronomical objects required very bright objects and exposure times lasting minutes.[17] Higher hole-burning efficiencies allow for a reduction of the exposure times and enable one to work with less bright

* Corresponding author. Telephone: +41 1 632 66 83. E-mail: plagemann@phys.chem.ethz.ch.

† Permanent address: Institute of Physics, EE2400 Tartu, Estonia.

S1089-5639(97)03353-7 CCC: $15.00
Published on Web 02/18/1998

light sources. In addition, higher hole-burning efficiencies reduce local heating, which can lead to unwanted enhanced spectral diffusion.[16,18]

An additional determinant of the frequency selectivity is the probability of zero-phonon transitions. The electron−phonon coupling makes the excitation of vibronic levels of the matrix possible.[19] This results in a broad feature in the absorption spectrum, the phonon sideband. The ratio of the integrated absorption cross section of all purely electronic lines (zero-phonon lines, ZPL) and the overall cross section is defined as the Debye−Waller factor (DWF). A high DWF is necessary for large-scale optical storage in order to avoid nonresonant effects and constitutes therefore an important issue in material optimization studies.

In recent studies the electric field has been used as an additional degree of freedom for spectral-domain multiplexing,[20,21] where the absorption frequencies are shifted upon application of an electric field due to the linear and quadratic Stark effect. The dipole moment difference between the ground and the excited state of the $S_1 \leftarrow S_0$ transition determines the amount of the shift and the feasibility for multiplexing.[20−25]

The long-term stability of the stored data is another crucial requirement. The back reaction of the photoproduct, which can occur spontaneously or can be induced by an increase of the temperature, leads to a loss of the signal quality of stored information. Thus, the long-term stability of spectral holes as well as the temperature-induced filling has to be examined.

Aiming at large-scale optical storage, the illumination of the complete spectral region of the inhomogeneous absorption band is involved. This can lead to laser-induced hole filling if the bands of the photoeduct and -product states are overlapping. To avoid this, the photoactive molecule should absorb in different wavelength regions before and after undergoing a photoreaction; that is, the educt and product state should be separated spectrally.

Some of the above-mentioned properties are correlated and cannot be optimized simultaneously.[26] The temperature dependence of some properties such as the DWF, the homogeneous width, and the hole stability necessitates the use of cryogenic equipment. Although the search for a high-temperature hole-burning material is a focus in current research,[14,27] we will restrict the investigations mainly to the liquid helium temperature regime. The molecule that has been mostly used so far, 2,3-dihydroporphyrin (chlorin), meets most of the requirements, except that it has a rather low hole-burning efficiency. Therefore, our main concern was to increase the hole-burning quantum efficiency and the absorption cross section while maintaining the spectral separation of the educt and product absorption.

1.2. Molecular Structure and Photochemical Properties. Several investigations have shown that the photochemical parameters depend on the structural characteristics of the pigments.[11,28,29] This is particularly true for metal-free tetrapyrrolic pigment molecules exhibiting NH tautomerization. The exchange of the two inner protons provides an efficient photochemical hole-burning mechanism,[28,29] and the scope of our investigation will be restricted to this class of materials.

It has been observed that a good separation between the educt and product state can be achieved by introducing asymmetry in the molecule.[29] Chlorin is a good example for this. The N−N axial inequivalence leads to a displacement of the ground- and excited-state potentials of the photoproduct. This may obstruct the transition from the intermediate triplet state to the photoproduct ground state and therefore reduce the hole-burning efficiency.[11] Symmetrical porphyrins, on the other hand, tend to have a much higher photochemical yield. The value can be higher by 2 orders of magnitude as compared with chlorin.[11] However, the spectral separation between the educt and product state is lost due to the identical structure of the two tautomers. As a result, the photoproduct absorption covers the same spectral region as the educt. This makes the use of centrosymmetric porphyrins for storage applications difficult because of the hole filling during the recording process. In other words, the spectral separation between the educt and product should be as small as possible to avoid the decrease of the photochemical yield, but large enough to ensure the spectral separation.

We noticed earlier that tetrabenzoporphyrin has a hole-burning quantum yield (Φ) as high as 7%.[30] The asymmetry can be introduced by replacing one of the benzene rings by a naphthogroup. In this paper we investigate the photochemical properties of the asymmetrically substituted tetrabenzoporphyrin at low temperatures. Since the properties of the compound have not been reported in the literature yet, we give a description of the synthesis and the basic spectroscopic features with an emphasis on those characteristics that are important for the application in optical data storage.

2. Experimental Section

2.1. Synthesis of Benzoporphyrins. The synthesis of zinc complexes of *meso*-phenyl-substituted benzoporphyrins was carried out according to ref 31. In short, a mixture of 0.56 g of potassium phthalimide, 0.2 g of 2,3-naphthalenedicarboximide (Aldrich), 1.4 g of potassium phenylacetate, and 0.32 g of zinc acetate was reacted for 30 min in a flow of dry nitrogen at 360 °C. The obtained mixture of green pigments was freed from dark contaminants by column chromatography on neutral Al_2O_3 (elution with $CHCl_3$−petroleum ether 1:1 v/v) and silica gel (elution with toluene). Zn was removed by adding a few percent of concentrated HCl to the solution of the pigments in *N*,*N*-dimethylformamide. Further separation of free-base porphyrins was performed on special SiO_2 thin layer chromatography plates having a nonadsorbing starting ("focusing") zone of Kieselgur (Silgur-25 UV_{254}, Macherey-Nagel, Switzerland), using a 3:1 mixture of toluene and petrol ether as an eluent. The lower and upper parts of the chromatogram (retention coefficients R_f = 0.55 (∼30%) and 0.77 (∼10%), respectively) belonged to tribenzonaphthoporphyrins with absorption maxima λ_m in *n*-heptane at 683.2 and 685.1 nm, respectively. The large middle fraction (∼60%) contains mainly the symmetrical compound with λ_m at 665.3 nm.

On the other hand, under similar conditions, a sample made only of potassium phthalimide yielded two main chromatographic zones, R_f = 0.66 (∼70%) and 0.78 (∼30%) with λ_m at 665.5 and 667.9 nm, respectively. It has been established that the high-temperature condensation reaction results predominately in *meso*-di- and *meso*-triphenyltetrabenzoporphyrins.[32] With the increasing number of *meso*-phenyl substituents the chromatographic mobility increases and the S_1 and Soret absorption maxima undergo a bathochromic shift.[32] Thus, we have concluded that the main asymmetric fraction (R_f = 0.55) is a mixture of *meso*-diphenyl-2,3,7,8,12,13-tribenzo-17,18-naphthoporphyrins (P_2TriBNP), with the phenyl groups at either two of the *meso*-positions of the tetrapyrrolic ring.

2.2. Sample Preparation. Poly(vinyl butyral-*co*-vinyl alcohol-*co*-vinyl acetate) (88% PVB, Aldrich) and an appropriate amount of the dye were dissolved in CH_2Cl_2, and the solution was filtered. The solvent was slowly evaporated in a Petri dish, yielding a thin film with good optical quality and a thickness

of 100−200 μm. The residual solvent was removed by heating at 80 °C in vacuum for several hours.

2.3. Absorption Measurements and Broad-Band Hole-Burning. Absorption spectra were recorded on a Perkin-Elmer Lambda 9 spectrophotometer. For low-temperature measurements it was equipped with a CF1204 continuous flow cryostat connected to a ITC-4 temperature controller (both Oxford). Holes were burned with a Lambda Physik dye laser LPD 3002E (line width 2.5 GHz, pulse length ~10 ns) pumped with an excimer laser LPX 100. The hole-burning quantum yields and Debye−Waller factors were estimated as described in ref 11. Holes were studied in transmission by scanning the dye laser with attenuated energy. In this case, detection was accomplished in a two-channel setup using a Molectron JD2000 joulemeter ratiometer with a sensitive J3S-10 (1 kV/mJ) probe in the sample channel and a less sensitive one, J3-09 (1 V/mJ), as a reference.[11] The instrumental contribution of 5 ± 0.5 GHz was subtracted from the measured hole widths.

2.4. High-Resolution Measurements and Holographic Detection. High-resolution measurements were performed at a temperature of 1.7 K, i.e., with the sample immersed in superfluid helium contained in a bath cryostat (Oxford MD10). The liquid provides effective cooling and has the advantage of a good optical quality. The absence of density fluctuations is particularly important for holographic applications. Narrow spectral holes were burned and probed with a single-frequency dye laser (Coherent CR899-29) with DCM as the laser dye. The ring laser was pumped by an Ar^+ laser and had a line width on the order of 1 MHz. The laser beam was expanded in order to make a homogeneous illumination and an accurate determination of the irradiance possible. The beam was then split in two parts. For the measurements requiring exact values of the absorbance, such as the determination of the DWF and the hole-burning efficiency, a reference beam passing only through the cryostat windows was monitored along with the expanded beam travelling through the sample. Signal detection was accomplished by means of two photomultipliers (Hamamatsu R 928). The experiments requiring a better signal-to-background ratio were performed with a holographic setup.[8,9] Here, both beams overlap on the sample during the burning period. Due to the photosensitivity of the medium, the resulting interference pattern forms an absorption/refractive index grating. During the readout, only one beam illuminates the sample. The light diffracted from the persistent holographic grating provides background-free detection with significantly improved signal-to-noise ratio. This technique was applied in the experiments dealing with low signal intensities such as the detection of shallow holes for the determination of homogeneous line widths or the measurements of hole shapes during the application of electric fields.

3. Results and Discussion

3.1. Absorption Spectra, Phototautomerism, and Broad-Band Hole-Burning of P_2TriBNP. New spectral bands appear in the absorption of tribenzomononaphthoporphyrin, P_2TriBNP, under illumination at 7 K (Figure 1). A large amount of the product absorbing at 641 and 675.5 nm is accumulated in the photostationary state upon irradiation at 614 or >680 nm. Figure 1 shows the spectra recorded with perpendicular polarizations of the probing light following an extensive bleaching of the 614-nm band with horizontally polarized laser light. Both the monitoring and reference beams of the spectrophotometer were rendered polarized by attaching two identical plastic polarizers on the exit windows. The photoselection measurement reveals that the 614-nm band of the educt and the prominent 641-nm band of the product have mutually perpendicular transition moments. On the other hand, both the bleaching of the 614-nm band and the increase of the $S_1 \leftarrow S_0$ absorption of the product at 675.5 nm are the strongest in the case of parallel polarization of the burning and recording light, suggesting that the respective transitions have the same direction.

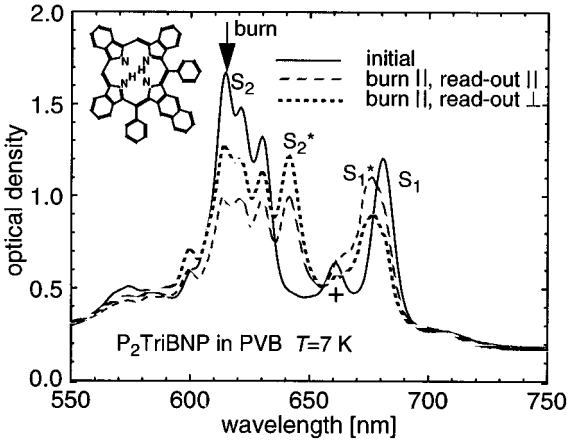

Figure 1. Photoselection experiment on the lowest two absorption bands of P_2TriBNP and its photoproduct in PVB at 7 K. The band marked with + belongs to the P_2TBP impurity. The transitions in the product state are starred. The S_2 band at 615 nm was irradiated with 0.6 J cm^{-2} fluence of horizontally polarized pulsed light. When detected with a vertically polarized light beam, the bleaching of the S_2 band is less, but the increase of the S_2* absorption is stronger and the S_1* absorption is less than those recorded with horizontally polarized light. The S_1 band of the educt is not discernible in the irradiated sample. The structure of P_2TriBNP is shown as an inset.

Monochromatic irradiation in the 600−650-nm wavelength interval results in very broad holes (10 ± 5 cm^{-1}) (data not shown). This can be associated with fast relaxation times (~1 ps) of the respective levels or very strong coupling to low-frequency vibrations. Tentatively, we assign the bands between 600 and 650 nm to the $S_2 \leftarrow S_0$ transition. The origin of the distinct bands of the educt at 614, 621, and 630 nm is not quite clear. Remarkably, such a triplet structure can be discerned also in the S_2 band of octaethylporphyrin at 530 nm. The assignment of spectral bands for both tautomers is illustrated in Figure 1. The transitions in the less stable form are denoted as S_1* and S_2*. As expected, the two Q transitions in both forms are perpendicular. Moreover, a photobleaching experiment of the S_1 band at 681 nm with polarized light shows that the S_1 and S_1* transitions are also perpendicular (data not shown). The absolute orientation of the transition moments remains unknown from these measurements. However, it will be shown below on the basis of Stark effect measurements that the symmetry axis and the S_1-S_0 moment are perpendicular in the educt.

As compared to phthalocyanines,[11] a naphtho substitution in P_2TriBNP leads to a relatively small shift between the S_1 and S_1* transition energies (400 cm^{-1} vs 115 ± 10 cm^{-1}). In this connection, it is of interest to note that the less stable tautomer has a hypsochromically shifted S_1 band in phthalocyanines and chlorins, whereas the opposite is true for porphyrin derivatives.[11] As it has been pointed out already for other asymmetric tetrapyrroles studied so far,[11] the average energy of S_1 and S_2 states in P_2TriBNP is close for both tautomers.

The photochemically accumulated product gradually disappears as the temperature increases (Figure 2). The educt half-recovery temperature (T_m = 91 ± 1 K) is only slightly lower than that for a (na)phthalocyanine (115 K) but considerably

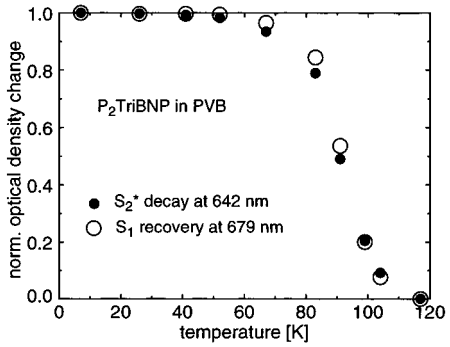

Figure 2. Normalized temperature-induced decay of the phototautomer and the recovery of the educt for P_2TriPNP in PVB monitored at the S_2* and S_1 absorption maxima, respectively. The photoproduct was accumulated at 8 K by scanning the pulsed dye laser over 613−616 nm with a total fluence of 1.5 J cm^{-2}. The S_1* and S_2* bands of the less stable tautomer disappear as the temperature increases. The half-decay temperature is 91 ± 1 K.

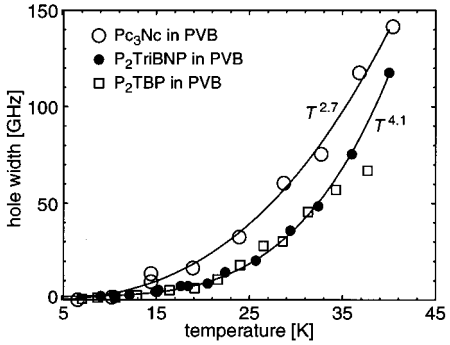

Figure 3. Temperature dependence of quasihomogeneous hole width in PVB doped with nonsymmetric (na)phthalocyanine, Pc_3Nc, nonsymmetric benzonaphthoporphyrin, P_2TriBNP, and symmetrical tetrabenzoporphyrin, P_2TPB. Lines represent the power-law fittings of experimental data, the temperature coefficient of which is indicated. Only the fitting curve for P_2TriBNP is shown.

higher than in chlorin (51 K).[11] About 10% of the thermally populated less stable tautomer of P_2TriBNP is present already at ambient temperature, showing up as a shoulder at ∼643 nm in the absorption spectrum. One can estimate from the Boltzmann distribution that the energy difference between the tautomers is ∼400 cm^{-1}. In the S_1 state the difference is larger by 115 cm^{-1} as the product absorption maximum (675.5 ± 0.5 nm in PVB at 8 K) is hypsochromically shifted.

The strength of electron−phonon coupling (EPC) may be characterized with the Debye−Waller factor (DWF) (linear EPC) and the temperature dependence of the quasihomogeneous hole width (Γ_{qh}) (quadratic EPC). A simple integration of the hole-burning spectrum yields the DWF for P_2TriBNP/PVB with a considerable error: 0.65 ± 0.07 at 7 K.

The number of reacted educt molecules divided by the amount of absorbed quanta gave the hole-burning quantum yield (Φ) estimate of 3.5 ± 1.5%. A more careful measurement of DWF and Φ described below resulted in very close values at 1.7 K.

The temperature (T) dependence of Γ_{qh} can be very well approximated to a power law with a T coefficient as large as 4.1 (Figure 3). Both the symmetric diphenyltetrabenzoporphyrin (P_2TBP) and nonsymmetric P_2TriBNP have identical hole widths. The holes in a (na)phthalocyanine derivative are considerably broader and show less steep T dependence ($T^{2.7}$).[11] This behavior is in accordance with very different dispersive solvent shifts in phthalocyanines ($p = -2000$ cm^{-1}, solvent shift in *n*-alkanes per unity Lorentz−Lorenz function at room T)[11,26,33] and benzoporphyrins ($p = -570 \pm 80$ cm^{-1} for fluorescence band maximum of parent TBP).[30] However, the T cycling study shows that the spectral diffusion contribution to the hole width is large or even predominant in P_2TriBNP. For example, at 20 and 30 K the $\Gamma_{qh}/2$ amounts to 5 and 19 GHz, whereas the broadening, induced by the warmup to these T's from 7 K and back (Γ_c), is as large as 3.5 and 14 GHz, respectively. Further, there is no increase of the DWF in P_2TriBNP expected on the basis of a small change of intermolecular interactions between the ground and excited states (small solvent shift), as compared to (na)phthalocyanines.[11,26] It seems probable that the *meso*-phenyl substituents, introduced to P_2TriBNP for better solubility and the ease of synthesis, may have torsional modes that contribute to the phonon wing. Also, the steric strain distorting the planarity of the π electronic system is definitely an unfavorable factor from the point of view of HB properties.

The narrow-band laser studies described in the following sections were carried out at 1.7 K with a PVB sample containing both the symmetric tetrabenzoporphyrin (P_2TBP) and the asymmetrical P_2TriBNP in approximately 1:1 ratio. The immersion of the sample in superfluid helium is necessary for use in practical applications since it permits the holographic detection of the spectral holes. The use of a codoped sample provided the opportunity to investigate both compounds in a single experiment under identical conditions.

3.2. Homogeneous Line Width and Debye−Waller Factor. The frequency selectivity of the material is determined by the ratio of the inhomogeneous width of the absorption band and the homogeneous hole width and by the DWF. The extrapolation to zero burning fluence and zero power yields an upper limit for the homogeneous line width.[34] Because of the time scale of the experiments, we could not observe changes in the line width taking place in times shorter than some seconds. To exclude broadening caused by the population of the triplet state and photochemical depletion of the ground state, a series of spectral holes was burned with constant burning time but varying irradiance. The signal-to-noise ratios for low light intensities were rather poor. Therefore, the holographically detected signals were used for the analysis.

The hole width increases linearly with the absorbed energy.[35] The width extrapolates to the same value at zero fluence for both the absorption holes and the holographic signals, which are defined as the ratio of diffracted and transmitted intensity.[35] A Lorentzian line was fitted to each hologram using a nonlinear least-squares method, and the full width at half-maximum and the respective standard deviation were determined. A weighted linear regression of the line width versus burning fluence was performed (data not shown). Only the initial linear regime was taken into account. The extrapolation to zero fluence yields a value of 236 ± 12 MHz or 0.008 cm^{-1} for the extrapolated hole width, which in turn corresponds to the double homogeneous width of the molecular absorption line. The inhomogeneous width of the S_1 band equals 230 cm^{-1}, which implies a ratio of inhomogeneous to homogeneous width on the order of 3×10^4.

The ratio of the widths of the inhomogeneously broadened absorption band and the homogeneous line is not the only parameter characterizing the frequency selectivity. Apart from the purely electronic transition, it is necessary to consider the contribution of vibronic levels in the dye-doped polymer.[19] The electron−phonon coupling leads to excitation of energetically higher levels than the purely electronic S_1 state, resulting in a broad feature in the spectrum denoted as the phonon sideband

or phonon wing. The DWF (α_{DW}) gives a quantitative measure for the impact of the linear electron−phonon coupling and is defined as

$$\alpha_{DW} = \sum_N \frac{\int_0^\infty \sigma_{ZPL}(\nu)\, d\nu}{\int_0^\infty \sigma_{total}(\nu)\, d\nu} \quad (1)$$

where the sum is over the entire ensemble of chromophores, σ_{ZPL} stands for the absorption cross section of the ZPL, and σ_{total} stands for the complete absorption feature of a single absorber. The summation of all absorption cross sections is represented by the inhomogeneous absorption band. We use a method to determine the DWF that can be applied in a high-resolution experiment rather than integrating the hole spectra of broad-band experiments as described before. One can distinguish experimentally between contributions of either the ZPLs or the phonon wing by investigating the burning kinetics. This is done by monitoring the absorption at a fixed frequency position while burning a deep spectral hole. From the kinetic data one extracts the initial optical density of the zero-phonon absorption and the extrapolated absorbance after infinitely long burning related to the phonon wing. Under the assumption of an optically thin sample, i.e., a constant light intensity through the sample, the time evolution of the chromophore density during the hole-burning process follows an exponential decay law. The convolution of the absorption profile with the time-dependent chromophore density yields the temporal evolution of the absorbance. The hole shape can be written as

$$A(\nu, t) = -A(t{=}0)\, \sigma_{ZPL}(\nu_b, \nu) \otimes N(\nu, t) \quad (2)$$

For identical frequencies of burning and probing one can calculate the convolution and take the value at the burn frequency ν_b. In addition, for long burning times the slow burning through the phonon wing is taken into account. Since the kinetics are much slower, we can approximate the corresponding decay of the optical density by introducing a linear decrease. Although the assumption of a constant intensity through the sample is rather crude, the crucial fit parameter is the contribution of the phonon wing to the optical density, which is not strongly influenced by this assumption. The initial optical density and the extrapolated value after infinitely long burning are extracted from fits to the data at various spectral positions. The shape of the absorption spectra of the molecules and the corresponding contributions of the phonon wings are approximated by Gaussian lines. The areas of the bands are obtained from the fit parameters. Because of the uncertainty in the baseline caused by long-ranging wings of the S_2 band, we can only determine a lower limit of the DWF for P_2TriBNP, yielding a value of 0.59.

3.3. Hole-Burning Yield and Triplet Lifetime. The photochemical hole-burning yield Φ is the most important parameter of this study. It is defined as the ratio of the number of photobleached molecules to the number of photons absorbed by the sample. One can write the hole-burning yield as

$$\Phi = \frac{dN/dt}{(1 - T')(1 - R)\alpha_{DW}F} \quad (3)$$

where N is the total number of absorbers per sample area, F is the photon flux per time, T' is the transmittance, and R is the reflectivity of the sample. α_{DW} accounts for the absorption by the phonon wing. The photon flux is obtained from the irradiance I at the burn frequency ν_b. The change of the number of molecules is calculated by comparing the area of spectral holes burned into the absorption band and the overall absorption. The total number of molecules absorbing in the wavelength interval under consideration is calculated from the molar extinction coefficient ϵ. The ϵ value for P_2TriBNP was assumed to be equal to that for P_4TBP in $CHCl_3$ ($2.5 \times 10^4\ M^{-1}\ cm^{-1}$), which was taken from the literature.[31] For the calculation of the areas of the absorption holes and the overall absorption band, respectively, we assume a Lorentzian line shape $L(\nu_b, \nu)$ for the spectral hole and a Gaussian shape $G(\nu_{max}, \nu)$ for the inhomogeneous band centered around the frequency ν_{max}.

It is assumed that the number of excited molecules and hence the area of the spectral hole increases linearly with the burning fluence. This holds for small holes and implies a constant transmission T'. The molecule concentration c can be calculated from the absorbance in the band center $A_{max} = c\epsilon d$, with d being the sample thickness. Therefore, we can rewrite eq 3 as

$$\Phi = \frac{h\nu_b}{(1 - T')(1 - R)\alpha_{DW}I} \frac{d}{dt}\left(\frac{\int_0^\infty L(\nu_b, \nu)\, d\nu}{\int_0^\infty G(\nu_{max}, \nu)\, d\nu}\right) \quad (4)$$

$$= \frac{h\nu_b A_{max}}{(1 - T')(1 - R)\alpha_{DW}I\epsilon} \frac{1}{A_{total}} \frac{d}{dt}\left(\int_0^\infty L(\nu_b, \nu)\, d\nu\right)$$

with A_{total} standing for the integrated absorption band, which is a constant value. The integral of the spectral hole is obtained by fitting a Lorentzian line shape function to the measured data. The area of the inhomogeneous band is determined by fitting a Gaussian function to the overall absorption of the S_1 band. A series of holes can be burned with increasing exposure time to calculate values for the hole-burning yield according to eq 4 from the obtained hole areas. Values for Φ have been determined at several positions in the inhomogeneous band. The evaluation yielded values with an average of $3.2 \pm 1.5\%$. The results increase almost by a factor of 2 going from the short- to the long-wavelength side of the band. Some uncertainties in the parameters used contribute to the error of the absolute value. We repeated the experiments with a chlorin-doped sample and determined the photochemical yield in the same way. The results show that the quantum efficiency for P_2TriBNP is higher by a factor of 50−100 than the value for chlorin. This corresponds to the results from the broad hole measurements reported above.

Apart from the photochemical hole-burning yield, there are further parameters determining the kinetics of the hole formation. Assuming that the molecule has a level scheme similar to other porphyrins,[36] the population of the first excited triplet state T_1 has to be considered. The lifetime of the S_1 state is on the order of 10 ns, as estimated from the homogeneous line width. The T_1 level has a much longer lifetime than the S_1 state and can be a bottleneck for the photochemical reaction.[37] The T_1 lifetime was measured by a transient hole-burning experiment using a pump−probe setup.[38] The change of the absorption of a weak probe beam is monitored during the switching of a stronger pump beam that is incident on the sample in the same area. The time constant of the exponential decay of the transparency of the sample after switching off the pump pulse can be identified with the lifetime τ_T of the level. A series of experiments yielded a value of $\tau_T = 5.9 \pm 0.6$ ms.

The extent of the power broadening of spectral holes depends on the lifetime of the T_1 state. As a result, the precondition of very fast creation of HB memories is the small triplet yield and

short τ_T. The requirements are exactly the opposite for the high burning yield, since the proton shift in free-base tetrapyrrolic pigments takes place on the T_1 potential surface.[11]

3.4. Dipole Moment Difference of the S_0 and the S_1 State. The influence of an externally applied electric field yields insight into the charge redistribution in a molecule taking place during the optical excitation. The difference of the dipole moments of a dye molecule in the ground and the first excited state can easily be measured. The method of spectral hole-burning in combination with the application of static electric fields has been developed in a number of previous publications.[20−25] Our investigations follow ref 24, which presents a complete description of the effects occurring, including the modeling of holographically detected signals.

The linear Stark effect produces a frequency shift $\Delta\nu$ in an external electric field $\mathbf{E}_S$ due to a difference of the dipole moments of the molecule in the ground and in the excited state $\Delta\boldsymbol{\mu}$ that can be calculated as

$$|\Delta\nu| = \frac{|\Delta\boldsymbol{\mu}||\mathbf{E}_S|f}{h}\cos\beta \qquad (5)$$

where h stands for the Planck constant, β for the angle between $\Delta\boldsymbol{\mu}$ and the electric field vector $\mathbf{E}_S$, and f for the Lorentz correction factor, which accounts for local electric field corrections in the amorphous matrix. It is given by $f = (\epsilon + 2)/3$, where ϵ is the low temperature dielectric constant, taken from ref 39.

The hole shape is measured holographically at different field strengths. Equation 5 gives the shift for a single absorber. To model the shape of the spectral hole, one has to average over an ensemble of molecules with a distribution of parameters caused by different orientations of the chromophores with respect to the external field, the polarization of the probing light, and the local matrix fields. The averaging has to be adapted to the type of molecule that is examined since the model assumptions are different, depending on the presence or absence of the molecular center of symmetry.

The molecule P_2TriNBP has an approximate symmetry group of C_{2v} and, therefore, should possess a permanent dipole moment in the ground state and in the first excited state. The dipole moment difference has a fixed direction with respect to the molecular coordinates. From the results of our measurements we must assume an additional matrix-induced component with a random orientation. The modeling of the data according to ref 24 must therefore include the fixed molecular, and the averaging over a randomly oriented, matrix-induced dipole moment difference. The averaging is done by calculating the theoretical hole shapes for different values and orientations of the matrix-induced component and weighting the resulting effective dipole moment difference with a Gaussian weighting function according to ref 23. The data analysis also includes the determination of the angle between the transition dipole moment and the fixed dipole moment difference.

This angle was determined to be 90°, and the resulting values for the dipole moment differences are 0.26 ± 0.03 D for the absolute value of the fixed dipole moment difference and 0.18 ± 0.02 D for the root mean square value of the matrix-induced contribution in the center of the absorption band. The calculated curves fit our data very well, as can be seen in Figure 4, and the determination of the field-induced frequency shifts is very accurate (less than 1%). Nevertheless, we estimate an uncertainty of the obtained molecular parameters of approximately 10%, which is mainly due to the uncertainty in the value of the sample thickness, which was determined by a capacitance measurement.

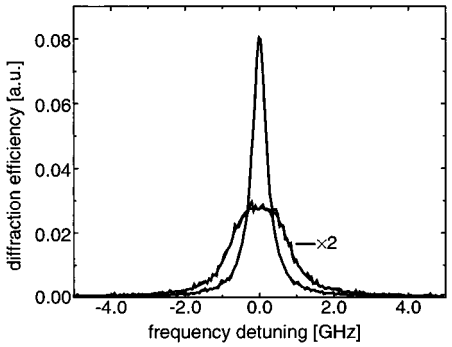

Figure 4. Broadening of a spectral hologram in P_2TriBNP/PVB (narrow) upon the application of an electric field of 2.7 kVcm^{-1} (broad) at 1.7 K. The hologram is burned in the center of the band at 683 nm. The curves could be fitted without systematic deviations only if both matrix-induced and permanent dipole moment differences are assumed. The splitting of the signal that becomes visible at higher field strengths is masked by the broadening caused by the matrix-induced contribution.

To check the validity of our model, we performed similar investigations in the absorption band of the symmetric P_2TBP. If one neglects the influence of the *meso*-phenyl groups, the P_2TBP molecule has D_{2h} symmetry and should be devoid of permanent dipole moments in either the ground or the excited state. Nevertheless, one observes broadening of spectral holes on application of an external field. The data analysis yielded a value of 0.20 ± 0.02 D for the width of the distribution of the matrix-induced dipole moment differences, which is similar to the result for the asymmetric compound. As expected, a permanent contribution could not be observed.

It is obvious from molecular symmetry considerations that the permanent dipole moments in P_2TriBNP should be oriented along the 2-fold axes passing the naphthopyrrole ring. Consequently, the $S_1 \leftarrow S_0$ transition dipole moment of the more stable prototropic tautomer passes the N atoms of the identical benzopyrrole fragments. The same nitrogens most probably carry the protons, as the negative charge density on the N atom in naphthopyrrole is less (see ref 11). Thus, as in the case of phthaloanthracenocyanine,[11] the transition dipole moment in P_2TriBNP passes through the N−H···H−N axes and turns by 90° together with the pair of protons upon tautomerization.

Hole broadening and particularly splitting in an externally applied electric field open interesting possibilities of manipulating optical memories.[20,21] Large dipole moment differences are favorable by allowing one to work at smaller voltages. Further, the inhomogeneous bandwidth strongly increases with increasing $\Delta\mu$,[26] which is potentially of great value in HB applications. Unfortunately, the strength of EPC is dramatically enhanced upon the increase of $\Delta\mu$.[26] Thus, in a polar oxazine dye, Nile Red ($\Delta\mu$ = 5 D), tiny holes can be burned at the very edge of the absorption band, indicating that the DWF has reduced to only several percent.[40] Also the quasihomogeneous hole width increases steeply along with $\Delta\mu$: a broadening by a factor of 4 has been observed in PVB at 1.7 K between chlorin ($\Delta\mu$ = 0.28 D) and isobacteriochlorin (1.2 D) or Cresyl Violet (2.1 D).[41]

3.5. Stability of Spectral Holes. The reliability of HB memories is mainly determined by the stability of the spectral holes. The time evolution of the hole area gives a quantitative measure for the stability of the photoproduct and the rate of the back reaction to the initial state. The measurements were performed with a holographic setup, and both transmitted and

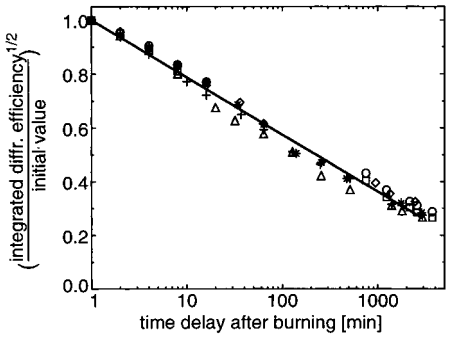

Figure 5. Time evolution of the area of five spectral holes in P_2TriBNP/PVB burned at different positions in the absorption band. The integrated areas of the holographically detected holes were normalized to the initial value taken 1 min after the burning. The straight line represents a logarithmic fit to the data according to eq 6.

diffracted signals were observed. The holographic signals were used for data evaluation because of the much better signal-to-noise ratio. The area decays with a logarithmic time dependence (Figure 5). This may correspond to a reverse reaction of the photoproduct with a distribution of back transfer rates that is correlated to two-level systems in the amorphous matrix.[42] The decay of the hole area A, normalized with the initial value A_i, can be expressed as

$$\frac{A(t)}{A_i} = 1 - \frac{\ln(R_i t)}{\ln(R_i/R_{min})} \qquad (6)$$

where R_{min} stands for the lower cutoff value of the occurring rates and R_i is the fastest value that is observed in the experiment. This number is in turn given by the inverse of the delay between the burning of the hole and the starting time of the observation t_i.

Assuming that the diffraction efficiency is proportional to the square of the corresponding hole depth,[43] one obtains the temporal area decay of an absorption hole of (21.2 ± 0.6)%/decade. The corresponding ratio of the rates (R_i/R_{min}) has a value on the order of 5×10^4.

This implies that in 3−4 h the area of a spectral hole is about a half the value that it had 1 min after the burning. This result appears to be in contradiction with the high thermal stability ($T_m = 91$ K) of the photoproduct accumulated at 7 K (Figure 2). It seems that at very low temperatures (1.7 K) some other nonphotochemical process with very shallow barriers can compete with the proton shift and/or the pigment molecule is trapped in cis form with adjacent protons in the ground state, which decays by tunneling of one of the protons (see ref 11).

3.6. Application in Holographic Storage. As mentioned previously, the investigated parameters of P_2TriBNP are crucial in determining whether or not it is suitable for optical data storage. Because of the large quantum yield of the phototransformation, the exposure times for the writing of information are reduced by at least 1 order of magnitude compared with the samples based on chlorin. We were able to detect spectral holograms with a contrast greater than 20 dB that were written with exposure times of only 100 ms (data not shown). The line widths showed only moderate power broadening. In a chlorin sample readout signals of comparable intensity would have required exposures of at least 2 s.

4. Conclusions

As a continuation of our studies aimed at the optimization of PSHB materials,[11,12] an asymmetrically substituted benzoporphyrin P_2TriBNP was synthesized, and the relevant spectral, photochemical, and electron−phonon coupling parameters were investigated. Regarding the crucial HB parameters a comparison was made with chlorin because it has been well-studied and used in different applications.[9,16,17] The Debye−Waller factor, the dipole moment differences, and the ratio of inhomogeneous to homogeneous line width of P_2TriBNP are rather similar to those of chlorin or even slightly better. The amount of the Stark splitting and broadening of spectral holes should allow similar electric field multiplexing as in chlorin and should result in information storage at approximately 10 electric field positions for each addressed frequency.

Most importantly, the photochemical hole-burning yield in P_2TriBNP is 2 orders of magnitude higher than in chlorin (3.2 ± 1.5% vs 0.03%). This brings about a drastic improvement as compared with the compounds used so far. It is of interest to note that further increase of light sensitivity of HB materials on the basis of one-quantum phototransformations does not make much sense since the recorded image is strongly bleached during the readout. Other organic molecules exhibiting PSHB capabilities, e.g. octaethylporphyrin, also provide a significantly higher yield than chlorin, but the photoproduct is not spectrally separated from the educt state because of the symmetry of the molecule. The spectral degeneracy of the educt and product absorption implies the disadvantage of laser-induced hole filling during the burning at many different positions throughout the absorption band. Moreover, the S_1 transitions in simple free-base porphyrins are relatively weak. The drawback of the proposed hole-burning system is that the back reaction rate of molecules transferred to the photoproduct state is rather high at 1.7 K, and the resulting hole filling limits the experimental time scale to several hours.

Nevertheless, the reduction of exposure times is an important step toward the technical implementation of such a device. One possible application that has recently been proposed is imaging spectroscopy of astronomical objects.[17] Here, both spatial and spectral information of the sun were recorded simultaneously in a one-shot experiment. The use of a material with a higher hole-burning yield renders the advantage of much shorter exposure times, leading to better spatial resolution, and it makes the investigation of objects with lower brightness possible. A second advantage is the reduction of the energy that is deposited in the sample during the recording of information. It has been shown that the absorption of high laser doses by the sample can cause additional broadening of previously burned spectral holes.[18] This light-induced spectral diffusion reduces the signal amplitude and therefore decreases the contrast of stored information. In a large-scale storage experiment, this can have an important impact on the signal-to-noise ratio.[16] The use of a system with a high photochemical yield and the possible reduction of the laser fluence needed by at least 1 order of magnitude would be an important step to overcoming this obstacle.

Acknowledgment. We thank Gregory Harms, Felix Graf, and Robin Purchase for stimulating discussions. Financial support from the Swiss CTI (Commission for Technology and Innovation), Project 2296.1, and support of the project "Spectral Hole-Burning in Optics" from the "Board of the Swiss Federal Institutes of Technology" and the Swiss Federal Institute of Technology Zurich is gratefully acknowledged.

References and Notes

(1) Gorokhovskii, A. A.; Kaarli, R. K.; Rebane, L. A. *JETP Lett.* **1974**, *20*, 216.

(2) Kharlamov, B. M.; Personov, R. I.; Bykovskaya, L. A. *Opt. Commun.* **1974**, *20*, 191.
(3) Moerner, W. E., Ed. *Persistent Spectral Hole Burning: Science and Applications*; Springer: Berlin, Heidelberg, 1988; and references therein.
(4) Macfarlane, R. M.; Shelby, R. M. In *Spectroscopy of Solids Containing Rare Earth Ions*; Kaplyanskii, A. A., Macfarlane, R. M., Eds.; Elsevier: Amsterdam, 1987; pp 51−184, and references therein.
(5) Szabo, A. U.S. Patent No. 3,896,420, 1975.
(6) Castro, G.; Haarer, D.; Macfarlane, R. M.; Trommsdorff, H. P. U.S. Patent No. 4,101,976, 1978.
(7) Renn, A.; Meixner, A. J.; Wild, U. P.; Burkhalter, F. A. *Chem. Phys.* **1985**, *93*, 157.
(8) Renn, A.; Wild, U. P. *Appl. Opt.* **1987**, *27*, 4040.
(9) Kohler, B.; Bernet, S.; Renn, A.; Wild, U. P. *Opt. Lett.* **1993**, *18*, 2144.
(10) Mitsunaga, M.; Uesugi, N.; Sasaki, H.; Karaki, K. *Opt. Lett.* **1994**, *19*, 752.
(11) Renge, I.; Wolleb, H.; Spahni, H.; Wild, U. P. *J. Phys. Chem.* **1997**, *101*, 6202.
(12) Renge, I.; Wild, U. P. *J. Phys. Chem.* **1997**, *101*, 4900.
(13) Völker, S. In *Relaxation Processes in Molecular Excited States*; Fünfschilling, J., Ed.; Kluwer: Dordrecht, 1989; Chapter 3.
(14) Reinot, T.; Kim, W.-H.; Hayes, J. M.; Small, G. J. *J. Opt. Soc. Am. B* **1997**, *14*, 602.
(15) Maniloff, E. S.; Altner, S. B.; Bernet, S.; Graf, F. R.; Renn, A.; Wild, U. P. *Appl. Opt.* **1995**, *34*, 4140.
(16) Plagemann, B.; Graf, F. R.; Altner, S. B.; Renn, A.; Wild, U. P. *Appl. Phys. B* **1998**, *66*, 67.
(17) Keller, C. U.; Graff, W.; Rosselet, A.; Gschwind, R.; Wild, U. P. *Astron. Astrophys.* **1994**, *289*, 41.
(18) Schulte, G.; Grond, W.; Haarer, D.; Silbey, R. *J. Chem. Phys.* **1988**, *88*, 679.
(19) Rebane, K. K. *Impurity Spectra of Solids*; Plenum: New York, 1970.
(20) Wild, U. P.; Bucher, S. E.; Burkhalter, F. A. *Appl. Opt.* **1985**, *24*, 1526.
(21) Bogner, U.; Beck, K.; Maier, M. *Appl. Phys. Lett.* **1985**, *46*, 534.
(22) Burkhalter, F. A.; Suter, G. W.; Wild, U. P.; Samoilenko, V. D.; Rasumova, N. V.; Personov, R. I. *Chem. Phys. Lett.* **1983**, *94*, 483.
(23) Bogner, U.; Schätz, P.; Seel, R.; Maier, M. *Chem. Phys. Lett.* **1983**, *102*, 267.
(24) Meixner, A. J.; Renn, A.; Bucher, S. E.; Wild, U. P. *J. Phys. Chem.* **1986**, *90*, 6777.
(25) Kador, L.; Haarer, D.; Personov, R. I. *J. Chem. Phys.* **1987**, *86*, 5300.
(26) Renge, I. *J. Opt. Soc. Am. B* **1992**, *9*, 719.
(27) Ehrl, M.; Deeg, F. W.; Bräuchle, C.; Franke, O.; Sobbi, A.; Schulz-Eckloff, G.; Wöhrle, D. *J. Phys. Chem.* **1994**, *98*, 47.
(28) Solovjev, N. N.; Zaleskii, E. I.; Kotlo, V. N.; Shkirman, S. F. *JETP Lett.* **1973**, *17*, 463.
(29) Mauring, K.; Avarmaa, R. *Chem. Phys. Lett.* **1981**, *81*, 446.
(30) Renge, I. Unpublished data.
(31) Kopranenkov, V. N.; Dashkevich, S. N.; Lukyanets, E. Ya. *Zh. Obshch. Khim.* **1981**, *51*, 2513 [*J. Gen. Chem. USSR* **1982**, *52*, 2165].
(32) Ichimura, K.; Sakuragi, M.; Morii, H.; Yasuike, M.; Fukui, M.; Ohno, O. *Inorg. Chim. Acta* **1991**, *176*, 31.
(33) Renge, I. *J. Phys. Chem.* **1993**, *97*, 6582.
(34) Thijssen, H. P. H.; van den Berg, R. E.; Völker, S. *Chem. Phys. Lett.* **1985**, *120*, 503.
(35) Meixner, A. J.; Renn, A.; Wild, U. P. *J. Chem. Phys.* **1989**, *91*, 67.
(36) Gouterman, M. In *The Porphyrins*; Dolphin, D., Ed.; Academic Press: New York, 1978; Vol. III, Chapter 1, pp 1−165.
(37) De Vries, H.; Wiersma, D. A. *J. Chem. Phys.* **1980**, *72*, 1851.
(38) Shelby, R. M.; Macfarlane, R. M. *Chem. Phys. Lett.* **1979**, *64*, 545.
(39) Altmann, R. B.; Renge, I.; Kador, L.; Haarer, D. *J. Chem. Phys.* **1992**, *97*, 5316.
(40) Vauthey, E.; Holliday, K.; Wei, C.; Renn, A.; Wild, U. P. *Chem. Phys.* **1993**, *171*, 253.
(41) De Caro, C.; Renn, A.; Wild, U. P.; Johnson, L. W. *J. Lumin.* **1991**, *50*, 309.
(42) Breinl, W.; Friedrich, J.; Haarer, D. *Chem. Phys. Lett.* **1984**, *106*, 487.
(43) Kogelnik, H. *Bell System Tech. J.* **1969**, *48*, 2909.